芸術科学会論文誌 Vol. 10, No. 3, pp. 118-128

A Study on Wind Turbulence Models for Animating Flexible Objects

Oyundolgor Khorloo[1] **Zorig Gunjee**[2] **Batjargal Sosorbaram**[1] **Norishige Chiba**[1]

[1] Iwate University [2] ECM LLC

[1]{oyuna@cg., batja@cg., nchiba@} cis.iwate-u.ac.jp [2]zorig@ecm.mn

風による柔軟物体の揺らぎ運動を表現する風乱流モデルに関する研究

ホルロー オユンドルゴール[1] グンジェー ゾリーグ[2] ソソラバラム バトゥジャルガル[1] 千葉則茂[1]

[1]岩手大学 [2]株式会社 ECM（モンゴル）

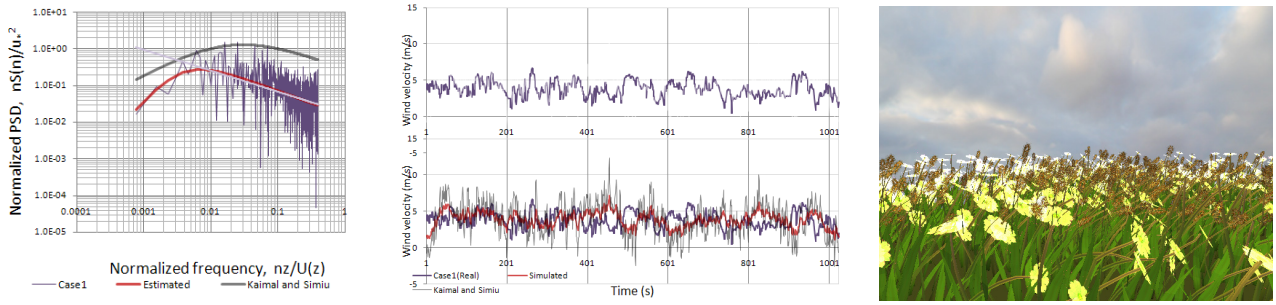

Figure 1. (Left) Actual wind spectrum compared with theoretical and estimated spectra; (Middle) Actual and simulated winds; (Right) Screenshot of grass field simulated using our approach

Abstract

A series of natural wind models have been developed since the 1960s to facilitate the study of wind engineering problems. In this paper, we present a study on wind turbulence models from the field of engineering and indicate their applicability in computer animations for simulating a variety of motions and the behaviors of flexible objects in windy conditions. We describe theoretical aspects of wind turbulence based on measurements of actual winds and their mean direction. We also describe a simple yet visually convincing simulation of wind fields using our proposed wind models generated from actual wind data. The efficiency and practical utility of the wind field model is implemented in a simulation of grass blowing in the wind.

Keywords: wind model, spectrum of turbulence, wind field simulation, grass animation

アブストラクト

風工学分野において，問題の取り扱いを容易にするために，1960年代以降，一連の風モデルが提案されてきた．本論文では，この風工学分野で研究されてきた乱流モデルについて述べ，それが風による柔軟物体の様々な揺らぎ運動のコンピュータアニメーションに適用可能であることを示す．まず，実際の風の実測データに基づき，風の理論的側面について述べ，次に風の実測データに基づいて得られた風のモデルによる，単純で視覚効果の高い風の場のシミュレーション法について述べる．最後に，風による草原の揺らぎ（穂波）現象に適用し，提案手法の効率性と有効性を示す．

キーワード:風のモデル、乱流スペクトル、風の場のシミュレーション、草原のアニメーション

1. Introduction

Wind is a very complex phenomenon because many flow situations can arise from the interaction between wind and objects. Thus, it is challenging to mathematically model wind. However, wind can be considered to possess stationary characteristics that can be described using statistical terms. Computer graphics has produced several wind models for simulating the motion of natural objects in wind. Most studies [e.g., 1, 2, 3, 4, 5] typically make use of stochastic approximations in wind modeling and consider simulations only in the frequency domain. To realistically model wind, experimental data and statistics can be used from other fields, e.g., structural engineering and wind engineering.

This paper is an extension of work originally presented at the NICOGRAPH Fall 2010. The main goal of this study was to construct a wind model using our data measurements of actual wind and employing theoretical approaches used in structural engineering. Structural engineering involves the study of strong winds that might cause damage and destruction of structures. In computer graphics applications, we need to realistically simulate different kinds of wind conditions such as breezes or gusts by controlling specific parameters in wind models. We also describe a simple approach for constructing wind fields with realistic turbulent winds that share similar characteristics with actual measured winds.

Figure 2 shows a general flow diagram of our proposed approach. This study included time history data collected for the mean wind speed in the Morioka area of Japan. As shown in Figure 2, we formulated a suitable wind turbulence spectrum in the frequency domain using theoretical approaches for wind engineering. Wind velocity time series were generated using the Fourier transform approach in conjunction with the proposed wind spectrum. We were able to generate winds with the requisite characteristics for use in time-domain response prediction of flexible objects, by employing the best-fitted formulation for the wind power spectrum.

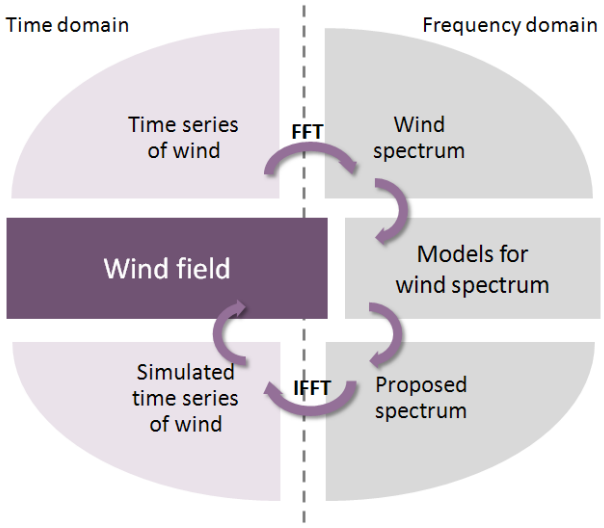

Figure 2. General flow diagram of our approach

The paper is organized as follows. We start with the experimental analysis of measured wind speed data using theoretical approaches from the structural engineering field. In section 2, we present the formulation and parameter estimates for our wind turbulence model using selected sample cases. In section 3, we present results of simulated winds determined with our proposed spectrum and we describe the implementation algorithm for constructing wind fields. Section 4 describes a simulation of grass fields utilizing our wind field method. Finally, we will conclude with the Discussion and Conclusions sections.

2. Analysis of data measurements

Mean wind speed time series were obtained for the Morioka area of Japan and used as an experimental basis for this fundamental study on wind modeling.

Table 1. Wind data measurements for Morioka area of Japan

	Date/Time	Terrain	z (m)	z_0 (m)	$U(z)$ (m s^{-1})	$\hat{U}(z)$ (m s^{-1})	σ_u (m s^{-1})	u_* (m s^{-1})	$I_u(z)$
Case 1	2009/07/06 5:08:03 PM	Suburban	3	0.3	3.81	6.7	1.1	0.66	0.28
Case 2	2010/03/13 3:51:40 PM	City	3	0.7	2.2	6.0	1.03	0.6	0.46
Case 3	2009/12/13 12:26:34 AM	City	3	0.7	1.16	3.5	0.68	0.31	0.79

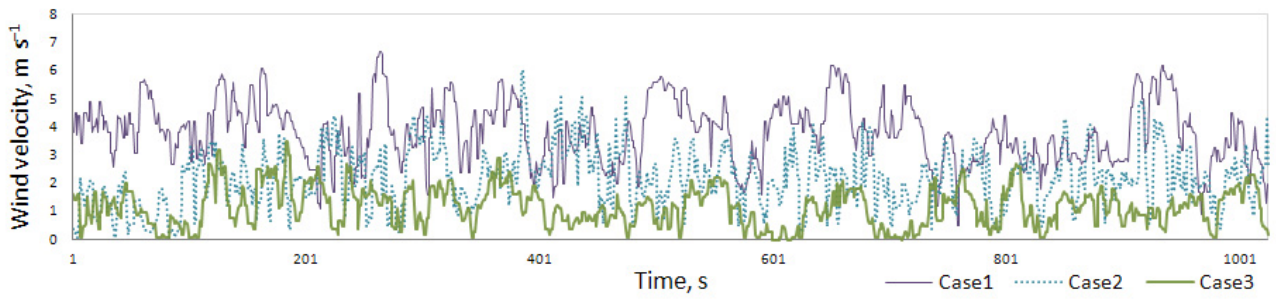

Figure 3. Time histories for sample cases

2.1 Measurements of mean wind speed

The wind speed data were collected with a hot-wire anemometer (Lutron, AM-4204) at a rate of 1 Hz. We selected three sets of data from the numerous wind samples based on the criteria that the sample cases can depict different wind characteristics in computer animations.

Each dataset had a sampling interval of 1 s and contained 1024 data points. The first case (Case 1) was measured in the suburbs at the top of a small hill, whereas other two cases (Case 2 and Case 3) were recorded around Morioka City, Iwate Prefecture. Time histories for the selected three cases are shown in Figure 3. All three cases were measured at a height of 3 m above the ground. Cases 2 and 3 shared the same terrain roughness with tall buildings and trees. The statistical measurements and estimates of the wind profile parameters for the selected cases are summarized in Table 1.

For each group, Table 1 lists the following: the date and time, terrain in each case, measured height above the ground, roughness length, mean wind speed U, maximum wind speed $\hat{U}$, dispersion σ_u, friction velocity u_*, and wind turbulence intensity I. Wind profile parameters are discussed in more detail in next section.

2.2 Wind profile parameters

Wind speed is affected by the frictional force caused by the terrain, near the ground surface. The mean wind velocity profile for the atmospheric boundary layer is described using a power law [6, 7]:

$$U(z) = U(z_{ref})\left(\frac{z}{z_{ref}}\right)^{\alpha} \tag{1}$$

where $U(z)$ is the mean wind speed at height z above the ground, z_{ref} is the reference height (normally taken to be 10 m), and α is the power law exponent.

An alternative description of the mean wind velocity uses the logarithmic law:

$$U(z) = \frac{1}{k} u_* \ln\left(\frac{z}{z_0}\right) \tag{2}$$

where u_* is the friction velocity, k is von Karman's constant (0.4), and z_0 is the roughness length. The determination of u_* from Eq. (2) requires $U(z)$, z, and z_0. The typical values for α and z_0 are listed in Table 2.

Wind blowing over the ground surface is slowed when it encounters the friction of uneven ground, trees, and buildings. This roughness affects the thickness of the boundary layer and the power law exponent. The thickness of the boundary layer and the power law exponent both increase as a function of the surface roughness. Thus, the velocity at any height decreases as the surface roughness increases. If the velocity of wind for a particular terrain is known, Eq. (1) and Table 2 can be used to calculate the velocity at some other terrain.

Table 2. Typical values for different terrains

	z_0	α
City centers	0.7	0.33
Suburban terrain	0.3	0.22
Open terrain	0.03	0.14
Open sea	0.003	0.10

In general, the velocity of wind may be represented in a vector form as

$$U(z,t) = U(z)i + u(z,t)i + v(z,t)j + w(z,t)k \tag{3}$$

where u, v, and w are the fluctuating components of the gust in x, y, and z directions (longitudinal, lateral, and vertical axes) and $U(z)$ is the mean wind speed along the x-axis.

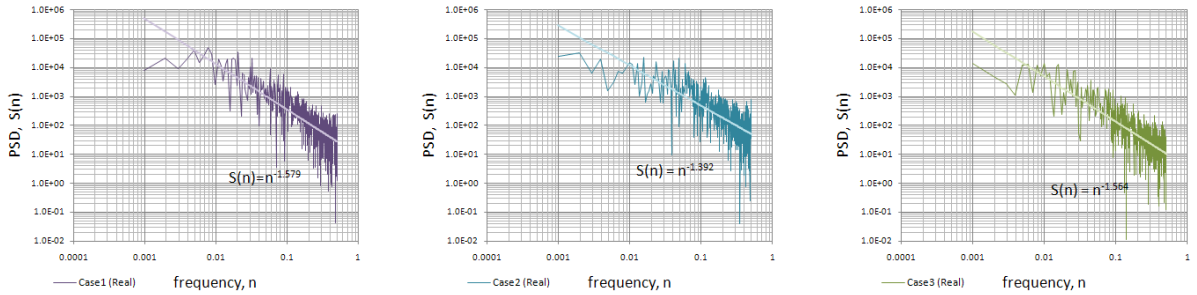

Figure 4. Power density spectra for sample cases

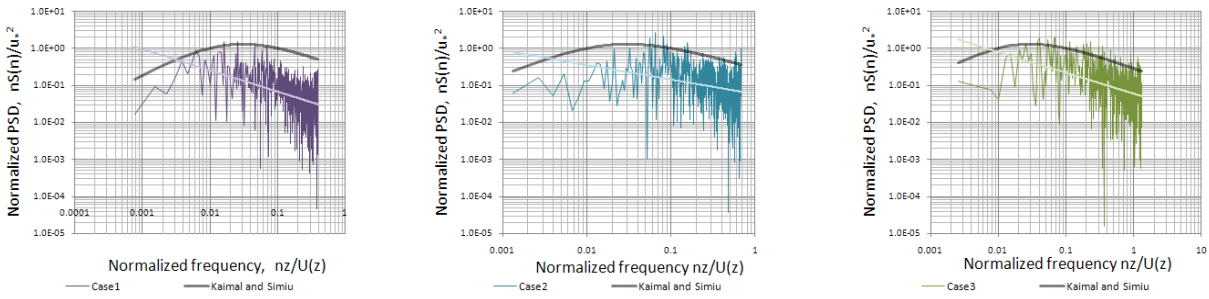

Figure 5. Normalized power spectra for sample cases compared with spectra of Kaimal and Simiu

The fluctuating component of the mean wind direction, u, is the largest and therefore the most important for structural engineering. Technical difficulties meant that we only studied wind velocity in the mean wind direction.

An overall measure of the intensity of turbulence is provided by the root mean square value. Thus, the longitudinal component of the turbulence is

$$\sigma_u(z) = \left[\frac{1}{T_0} \int_0^{T_0} u^2(z,t) dt \right]^{1/2} \tag{4}$$

where T_0 is the averaging period.

The value of $\sigma_u(z)$ divided by the mean velocity U(z) is called the turbulence intensity.

$$I_u(z) = \frac{\sigma_u(z)}{U(z)} \tag{5}$$

This value increases with ground roughness and decreases with height. The estimated values for the corresponding wind profile parameters in our sample cases are listed in Table 1.

2.3 Spectrum of wind turbulence

The power spectral density (PSD) function, also referred to as a power spectrum, is another important function for describing the characteristics of wind. A spectral density function is denoted by $S_u(n)$, where the variable n is the frequency. In each case, we computed the square of the amplitude, $A^2(n)$, using the fast Fourier transform (FFT). The power spectral density of the wind velocity is calculated as $S(n) = A^2(n)/\Delta n$, where Δn is the sampling frequency f_s multiplied by the number of data points N used in the FFT. Figure 4 shows the power spectra using the log-log method for our sample cases. As shown in Figure 4, the logarithmic slopes of the spectra are different, depending on the characteristics of the winds and terrains. The relationship between $S_u(n)$ and n appears as a straight line in this graph. In Case 1, $S_u(n)$ is proportional to $n^{-1.579}$ in the inertial subrange portion of the spectrum, whereas $S_u(n)$ is proportional to $n^{-1.392}$ in Case 2.

There are many mathematical models of wind power spectra [8, 9, 10, 11, and 12]. The purpose of this study was to produce a suitable wind turbulence spectrum from our measured data by considering different forms of spectral density used for describing wind turbulence. Wind power spectrums are expressed in a non-dimensional form, so we computed normalized power spectral density $nS(n)/u_*^2$ and normalized frequency $nz/U(z)$.

In this section, we present a comparative study of these spectral densities. The formulae for the spectral densities are summarized as follows.

1. Kolmogorov [6]

$$\frac{nS_u(n)}{u_*^2} = 0.26 f^{-2/3} \tag{6}$$

where n = the frequency in hertz,
u_* = the friction velocity,
$f = nz/U(z)$ is the reduced frequency,
$U(z)$ = the mean wind speed at height z.

2. Davenport [10]

$$\frac{nS_u(n)}{u_*^2} = \frac{4.0x^2}{(1+x^2)^{4/3}} \tag{7}$$

where $x = 1200n/U(z)$

3. Kaimal [11] and Simiu [12]

$$\frac{nS_u(n)}{u_*^2} = \frac{200f}{(1+50f)^{5/3}} \tag{8}$$

where $f = nz/U(z)$

The turbulence spectral density functions formulated to date have specific advantages and drawbacks. For example, Davenport's spectrum has no relationship with height above the ground, whereas the spectrum proposed by Kaimal and Simiu depends on the altitude and it can be applied to both low-frequency and high-frequency spectrum areas.

Figure 5 shows a comparison between the theoretical spectral densities for the measured wind power spectrum in our sample cases. Comparison of the wind spectrum of the measured data and the theoretical power spectra indicated that the wind spectrum extracted from the measured data did not closely match the spectrum proposed by Kaimal and Simiu. Therefore, we constructed the wind speed spectrum using our measured data because it provided an advantage for wind simulations in computer animations.

2.4 Parameter estimation for wind power spectrum model

In order to develop a more suitable wind power spectrum for our measured data, we consider a more general form of spectrum model suggested by Olesen et al. [13].

$$\frac{nS_u(n)}{u_*^2} = \frac{Af^{\gamma}}{(1+Bf^{\alpha})^{\beta}} \tag{9}$$

To determine the unknown coefficients A, B, α, β, and γ, we applied the following four criteria from [13] to the model:

(I) $\gamma - \alpha\beta = -2/3$

(II) $f_m = \left(\frac{1.5\gamma}{B}\right)^{1/\alpha}$

(III) $G_m = A\left(\frac{1.5\gamma}{B}\right)^{\gamma/\alpha}(1+1.5\gamma)^{-\beta}$

(IV) $\frac{\sigma^2}{u_*^2} = \frac{1.5A}{B}$

where f_m is the observed position of maximum and G_m is the observed value of the maximum.

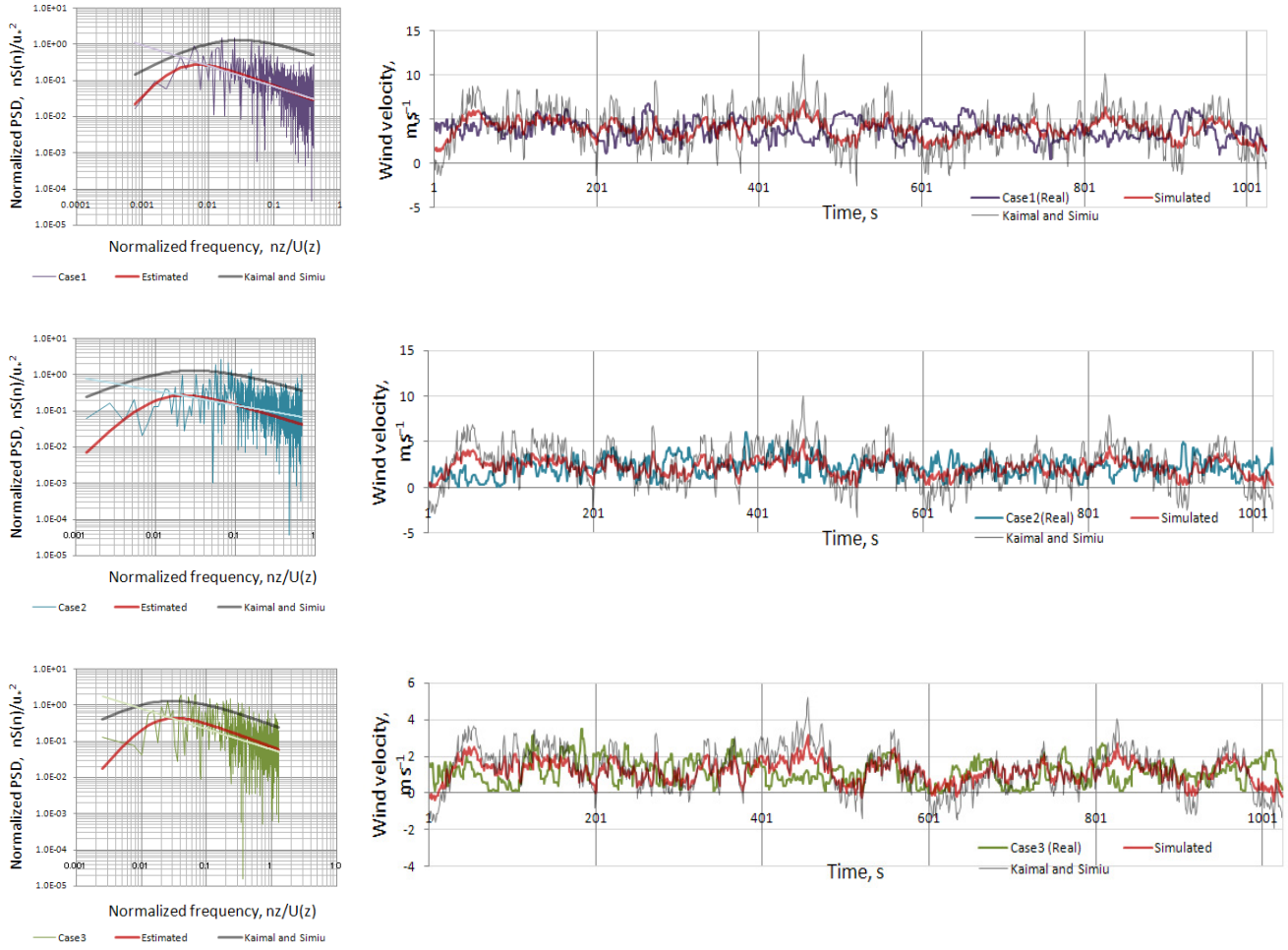

Figure 6. (Left) Proposed spectrum with spectrum of Kaimal and Simiu and the original wind spectrum for each sample case; (Right) Simulated winds for each sample case

The first criterion determines the slope of a high-frequency asymptote, according to Kolmogorov's law. The second and third criteria provide observed positions and observed values where the model maxima coincide. The fourth criterion is called the integral criterion. A and B determine the spectral frequency range, whereas α, β, and γ determine the spectral shape.

Using these criteria, a total of five unknowns are reduced to two unknowns. The remaining two unknowns are approximated using the Gauss-Newton iterative algorithm until the best agreement between the original and proposed spectra is reached. The estimated values of parameters for our data cases are listed in Table 3.

Figure 6 shows the proposed spectrum estimated using the corresponding parameter values listed in Table 3.

Table 3. Estimated values of parameters

	A	B	α	β	γ
Case 1	83762	20941	1.78	1.57	2.1
Case 2	8283	2071	1.70	1.62	2.1
Case 3	5314	1329	1.77	1.56	2.1

As shown in Figure 6(a), the proposed spectrum of wind turbulence for Case 1 has a peak value at a very low frequency of around 0.006 Hz, whereas the spectrum suggested by Kaimal and Simiu has a peak value at 0.02 Hz.

3. The proposed method

3.1 Wind simulation

The time series simulation of wind velocity fluctuations produced in our study uses the best-fitted wind power spectrum extracted from our measured data. Any random signal with varying frequency can be represented using the FFT method [14, 15]. The Fourier coefficients associated with this FFT are obtained using Gaussian random numbers, with zero mean and a specific standard deviation. We set the standard deviation of randomly generated numbers to the same as those found in the measured wind velocity data.

In the previous section, we formulated a wind power spectrum for a general case and estimated turbulence spectrum parameters. Hence, our generated wind velocity time series will be characterized by their spectral densities as

$$S_u(n) = \frac{u_*^2 A f^{\gamma}}{n(1 + Bf^{\alpha})^{\beta}} \quad (10)$$

where $f = nz/U(z)$.

We added the steady mean wind component (slowly varying component) after calculating the longitudinal wind turbulence from the mean wind speed.

Figure 6 shows the simulated wind time series for the measured wind time histories. Figure 6 shows that the simulated wind constructed with the spectrum of Kaimal and Simiu [11, 12] has a larger variation from the measured data and our estimated data. The wind velocity simulation generated using our proposed estimation had similar wind characteristics to that found in the measured wind velocity data.

A consideration of wind profile parameters such as measured height above the ground, mean wind speed, roughness length, and frictional velocity in the estimation of wind turbulence spectrum provides a better approximation in the simulation of wind.

3.2 Wind field construction

Wind engineering commonly uses algorithms to simulate turbulent windy fields, which are based on a model of the spectra for atmospheric surface-layer turbulence during high winds. Generally, it is possible to simulate two- or three-dimensional fields using one, two, or three components by employing empirical forms of one-point spectra. The data analyzed for this part of the study consisted of velocity measures at a single point with a turbulent flow fluctuation.

We ignored spatial correlations between points in order to simplify the simulation of wind velocity fields. Overall, two-dimensional velocity fields were simplified into many one-dimensional velocity fields. Thus, our approach for constructing wind fields considered wind-speed time series at several points in a plane perpendicular to the mean wind direction, which propagated the time series in the mean wind direction at the mean wind speed (using Taylor's frozen turbulence hypothesis). For the sake of simplicity, we construct two-dimensional wind fields containing two components of the wind velocity fluctuations. For the longitudinal component of the wind turbulence, we applied the estimated wind power spectrum because it fits well with our measured data, as shown in the previous section.

Technical constraints meant that the spectrum of the horizontal-lateral component of wind turbulence, $v(t)$, used Eq. (11), as suggested by Kaimal et al. [11] and slightly modified by Simiu and Scanlan [6].

$$\frac{nS_v(n)}{u_*^2} = \frac{15f}{(1+9.5f)^{5/3}} \quad (11)$$

where $f = nz/U(z)$.

Generally, any given wind field can be described using the long-term change and short-term change in the velocity field. The long-term change in velocity is determined by steady mean flow and long-term fluctuation of velocity. The short-term change in velocity is characterized using the turbulence spectrum of the wind. Thus, we investigated steady mean flow based on the short-term turbulence.

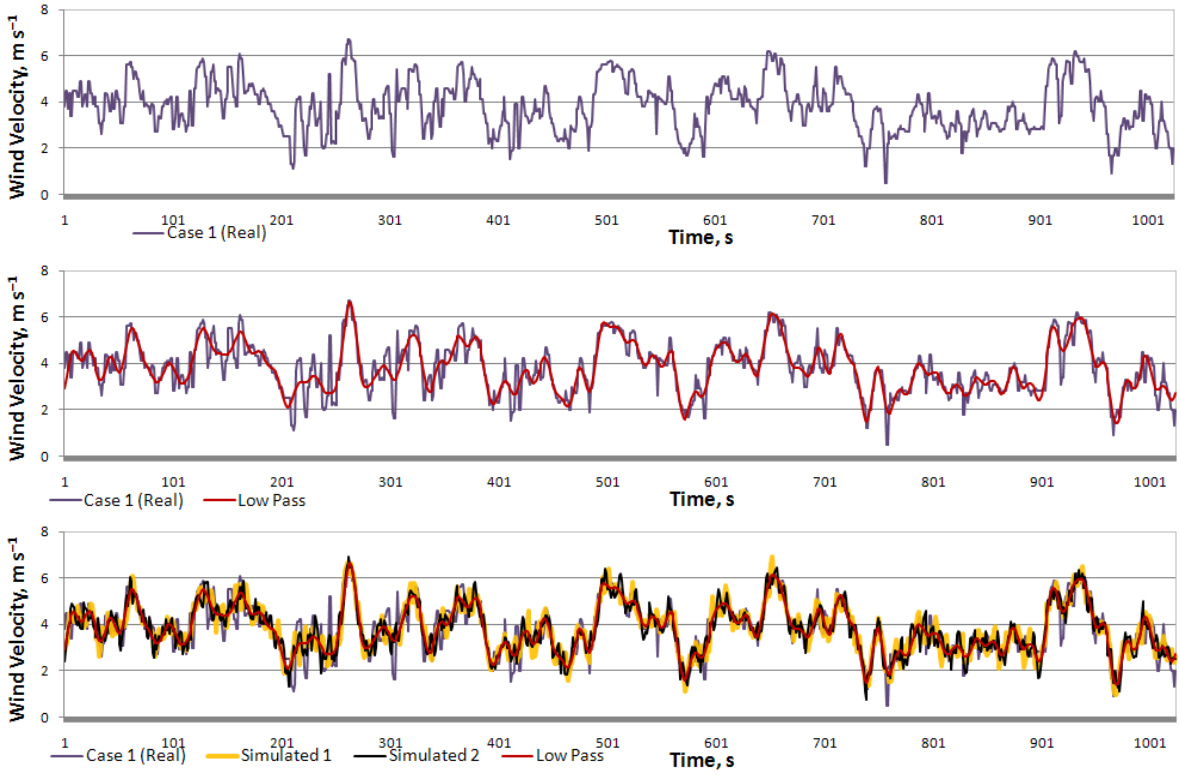

Figure 7. Steps in wind field simulation: (Top) actual wind history, (Middle) result of low-pass filtering, and (Bottom) simulated winds at two different locations

The long-term history of wind fluctuations can be set by the animators in a practical animation. In this study, we used a low-pass filter of the observed spectrum from our measured data to determine the long-term history of the wind. Short-term turbulence of the horizontal longitudinal component near the surface was computed using Eq. (10) with the estimated parameters listed in Table 3.

The implementation steps for the wind field simulation are described as follows.

Step 1: Estimate the longitudinal velocity spectra from the measured data at a single point.

1. Initialize 1D data array using the measured wind speed data, with a mean of 0.
2. Evaluate PSD, $S_u(n)$ in the spectral domain by applying 1-D Fourier transform.
3. Calculate friction velocity u_* using Eq. (2), with a given mean wind speed, roughness, and height measured above the ground.
4. Evaluate the normalized PSD, $nS_u(n)/u_*^2$.
5. Estimate parameters A, B, α, β, and γ in Eq. (9), for the given criteria.

Step 2: Evaluate the wind turbulence spectrum for each wind velocity component. For the 2D wind velocity field:

1. Initialize the 2D array $S_u[M][N]$ with a longitudinal velocity spectrum given by Eq. (10), to simulate a wind time series of length N at M different locations.
2. Initialize the 2D array $S_v[M][N]$ with a horizontal lateral velocity spectrum given by Eq. (11).
3. Multiply random phase $exp(\varphi)$ by both $S_u[M][N]$ and $S_v[M][N]$, where φ is a uniform random number from $-\pi$ to π.

Step 3: Determine the long-term history of the fluctuation.

1. Apply the measured wind spectrum calculated in Step 1 (3), to determine the long-term fluctuation of the wind history.
2. Replace the longitudinal velocity spectrum, S_u, with the measured wind spectrum for very low frequencies.

Step 4 Apply 1-D inverse Fourier transform M times for each wind component:

- IFFT1D(S_u)
- IFFT1D(S_v)

Once we determine the long-term history from our measured data, our simulated field is strongly correlated in the low-frequency range and there are random fluctuations in the higher frequency range. The variation of the fluctuations will be very similar to the measured wind velocity. Simulated winds at two different locations are shown in Figure 7. We generated a correlated time series with a length of N = 1024 at two different locations in the simulation of wind fields for sample Case 1. The simulated wind field is shown in Figure 8. We assumed that the selected number of positions were perpendicular to the direction of the mean wind.

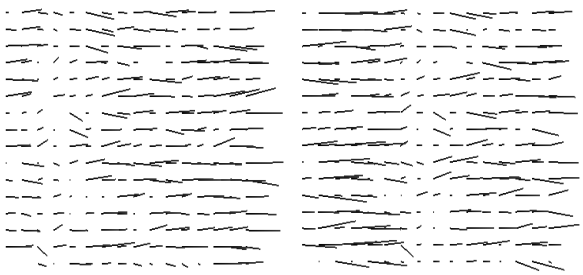

Figure 8. Simulated wind fields for sample Case 1 when $M = 16$ and $N = 16$ (Turbulence travels in the mean wind direction).

The time consumption for the overall steps is proportional to the total number of locations M in the simulation. The time required to perform the FFT is $O(N \log_2 N)$.

4. Grass field animation

To simulate the effects of wind turbulence on flexible objects, we considered a field of grass blowing in the wind. Our purpose was to simulate grass that waves realistically in the wind.

4.1 Grass model

In this section, we describe a simple yet visually convincing grass simulation based on our wind field model described in the previous section. We considered detailed modeling of individual blades of grass in this study. For large meadows, this will of course require large number of polygons.

Here, we apply a simple but useful solution that meets the condition of representing the deformation caused by the influence of wind velocity. In our grass field simulation, grass blades were built using the Bantam3D Grass application [16]. This application easily creates ground cover and stores the data in an object file format. A standard grass blade is copied many times to create the ground cover. We made the copies look slightly different from each other, in order to simulate nature. A grass blade is defined by

- the curve of the grass blade
- the size and rotation
- the color of the blade

Samples of ground cover created using the Bantam3D Grass application are shown in Figure 9.

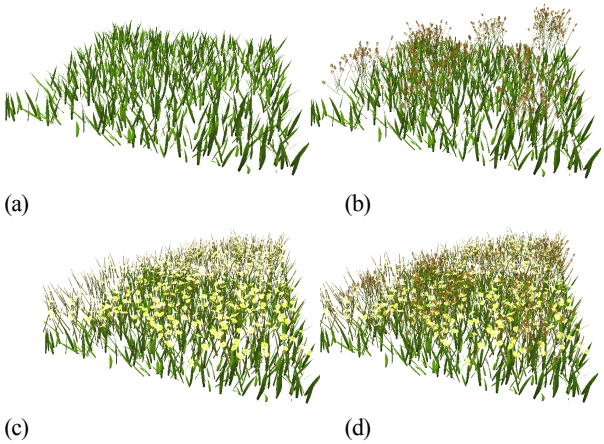

Figure 9. Ground covers created using Bantam3D Grass application

The parameters of created ground covers for Figure 9 are summarized in Table 4.

Table 4. Parameters for Figure 9

	Object type	Num. of nodes / obj.	Num. of objects
Figure 9(a)	Grass blade	6	1000
Figure 9(b)	Grass blade	6	1000
	Wheatgrass blade	12	500
Figure 9(c)	Grass blade	6	1000
	Daisy white flower	12	1000
Figure 9(d)	Grass blade	6	1000
	Wheatgrass blade	12	500
	Daisy white flower	12	1000

4.2 Grass animation

In order to achieve a highly realistic animation, we used a calculation based on our simulated wind field. This calculation also took into account the position to be moved. The direction and strength of the prevailing wind were also important factors. Lower points of the blades are fixed at a given location, whereas the upper points are shifted in the mean wind direction by the estimated wind velocity.

The middle points of the blades control the deflection and bending of the grass blade depending on the transition of the upper points. We wanted to draw numerous grass blades at one time, so the blades had to vary from time to time to make the grass blades look slightly different. Therefore, we applied different shades of green and yellow to provide a better differentiation of single blades.

A linear arrangement of grass blades would immediately make the structure recognizable. Therefore, we positioned the grass blades randomly. The length of the grass blades was also chosen randomly. In the simulation of grass animation, we did not consider stiffness and the clumping of grass blades for the sake of simplicity.

We use Taylor's frozen turbulence hypothesis to interpret a time series as a space series. Taylor's hypothesis is a widely accepted assumption and can be expressed for the two-dimensional case as follows:

$$u(x,y,t) = u(x - tU, y, 0) \tag{12}$$

The advantage of using this hypothesis is that the dimensionality of the data can be reduced from three to two.

As stated in Section 1, our measured data was collected at a height of 3 m above the ground. Therefore, we decreased the wind velocity at the height of grass based on Eq. (1) in the grass animation. Animation frame sequences of the grass field for the sample Case 1 is shown in Figure 10. Figure 11 shows screenshots of grass fields from various view angles. The accompanying video illustrates the real-time simulation of the grass field blowing in the wind.

4.3 Performance results

We chose a grass field to visualize wind fields simulated by our approach. In our grass field animation, we considered three kinds of grass blades as shown in Figure 9. From the experiments, our simulated grass field illustrates effects that are very similar to natural grass fields.

Computational performance for Figure 9 is as follows: (a) 64.85, (b) 61.93, (c) 34.28, (d) 23.71 (fps). The computer environment used was a 3.0 GHz Intel Core 2 CPU, with a NVIDIA GeForce 9400 GT video card and 2GB of memory.

5. Discussion and Conclusions

- This paper was mainly concerned with the characteristics of wind velocity near the ground. We determined the wind turbulence of the longitudinal wind component based on an examination of the wind spectrum and explored theoretical approaches from structural engineering for evaluating experimental wind profile data. Finally, we constructed wind velocity time history data based on the proposed wind power spectrum.
- In computer animations, motion simulation in wind fields is constructed using stochastic approaches or statistical models applied in the field of structural engineering. This is not an ideal approximation of a specific wind with a certain profile because of the varying conditions of the atmosphere and terrain. Thus, better estimation of wind profile parameters is important in wind simulations.
- We constructed a wind field with the same characteristics as the real wind measurements that our wind turbulence model was based on, and simulated wind fields exhibiting the motion of grass waving in the wind. A user can view and manipulate grass motions in real time by changing the profile parameters of the wind. Our technique can be further extended to other flexible structures.

Acknowledgement

This work was partially supported by the research grant from TOSTEM Foundation for Construction Materials Industry Promotion.

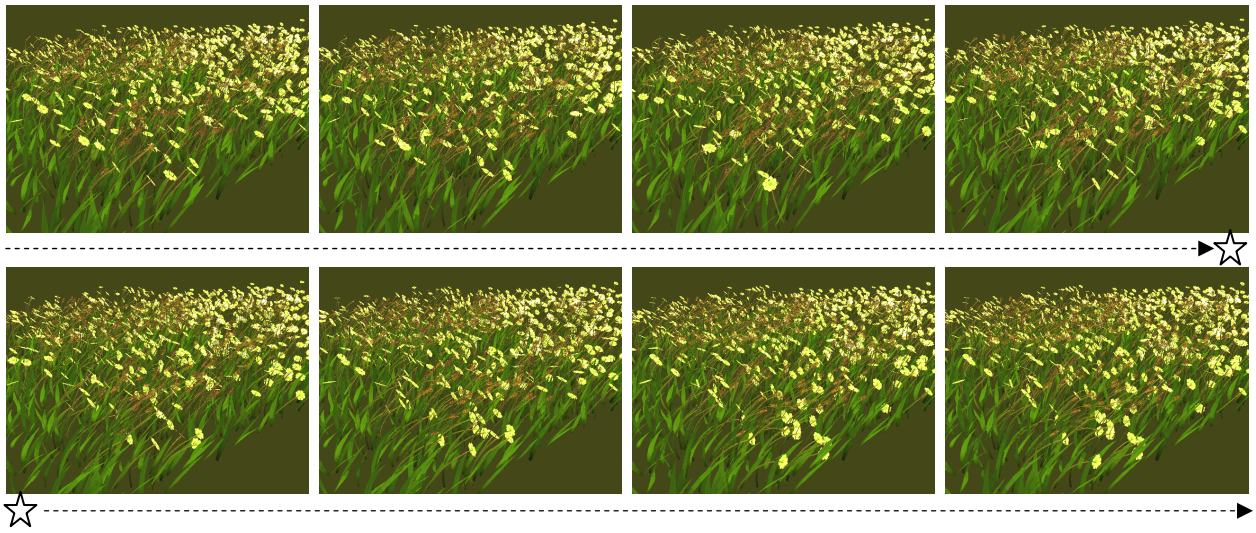

Figure 10. Animation frame sequences of the grass field

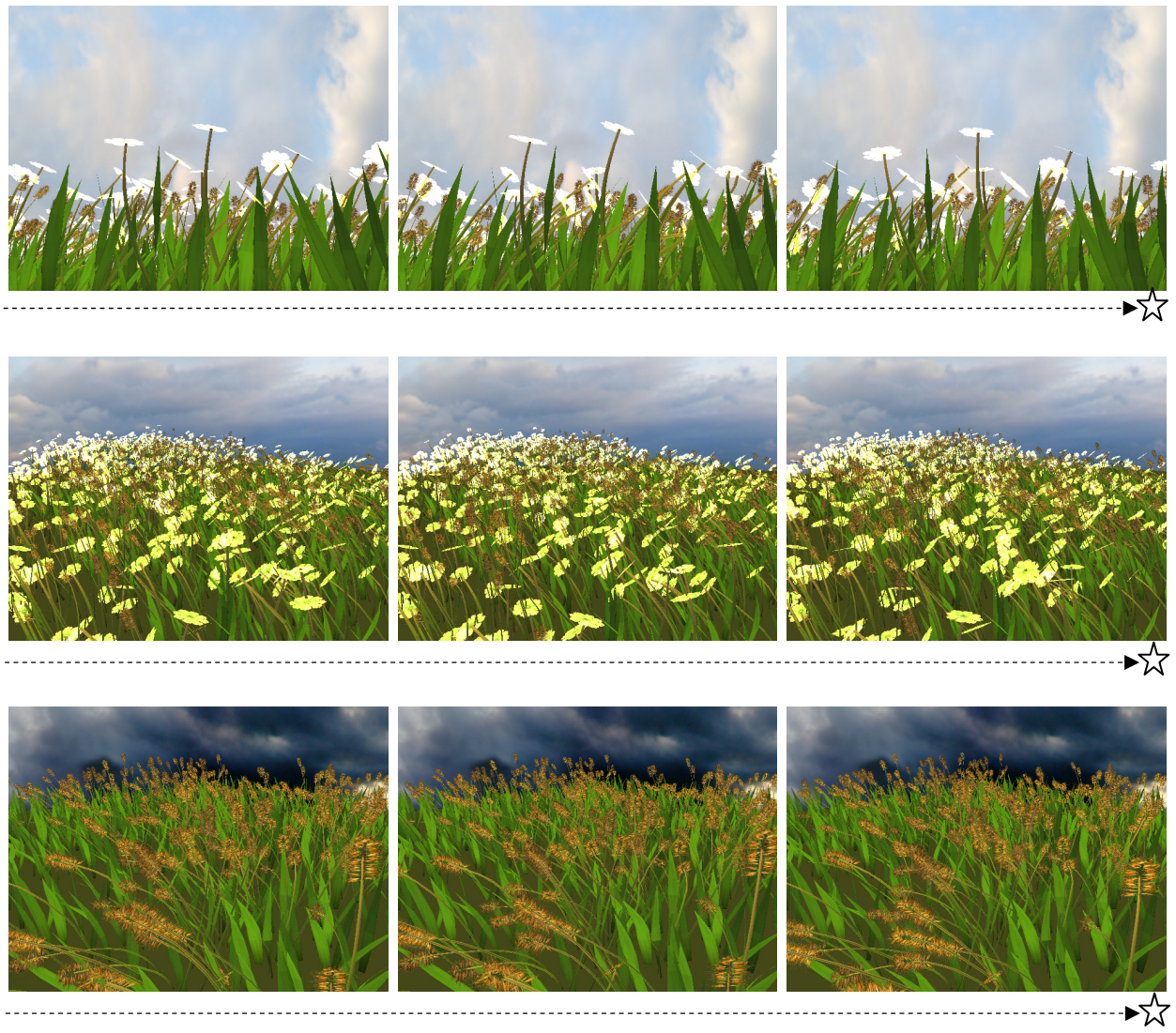

Figure 11. Grass fields from different view angles

References

[1] M.Shinya, A.Fournier, Stochastic Motion – Motion under the Influence of Wind, In Proceeding of Eurographics'92, pp. 119-128, 1992.

[2] J.Stam, Stochastic Dynamics: Simulating the Effects of Turbulence on Flexible Structures, Computer Graphics Forum, Vol. 16, No. 3, pp. 159-164, 1997.

[3] M.Sun, A.D.Jepson, E.Fiume, Video Input Driven Animation (VIDA), In Proceedings of IEEE International Conference on Computer Vision (ICVV), pp. 96-103, 2003.

[4] Y.-Y.Chuang, D.B.Goldman, K.C.Zheng, B.Curless, D.H.Salesin, R.Szeliski, Animation Pictures with Stochastic Motion Textures, In SIGGRAPH, pp. 853-860, 2005.

[5] R.Habel, A.Kustering, M.Wimmer, Physically Guided Animation of Trees, Computer Graphics Forum, Vol. 28, pp. 523-532, 2009.

[6] E.Simiu, R.H.Scanlan, Wind Effects on Structures, 2nd Edition, John Wiley and Sons, Inc., New York, 1986.

[7] J.D.Holmes, Wind Loading of Structures, Spon Press, London, 2001.

[8] J.Jang, Y.Lee, A Study of Along Wind Speed Power Spectrum of Taiwan Area, Journal of Marine Science and Technology, Vol. 6, No.1, pp. 71-77, 1998.

[9] D.Hiriart, J.L.Ochoa, B.Garcia, Wind Power Spectrum Measured at the San Pedro Martir Sierra, Revista Mexicana de Astronomia y Astrofisica, Vol. 37, pp. 213-230, 2001.

[10] A.G.Davenport, The Spectrum of Horizontal Gushiness near the Ground in High Winds, Journal of the Royal Meteorological Society, Vol. 87, pp. 194-211, 1961.

[11] J.C.Kaimal, Spectral Characteristics of Surface Layer Turbulence, Journal of the Royal Meteorological Society, Vol. 98, pp. 563-589, 1972.

[12] E.Simiu, Wind Spectra and Dynamic Along-Wind Response, Journal of the Structural Division, ASCE, Vol. 100, No. 9, pp. 1897-1910, 1974.

[13] H.R.Olesen, S.E.Larsen, J.Hojstrup, Modeling Velocity Spectra in the Lower Part of the Planetary Boundary Layer, Boundary-Layer Meteorology, Vol. 29, pp. 285-312, 1984.

[14] B.B.Mandelbrot, The Fractal Geometry of Nature, W.H.Freeman and Company, New York, 1982.

[15] R.F.Voss, Fractals in Nature: From Characterization to Simulation, in The Science of Fractal Images, edited by H.O.Peitgen and D.Saupe, Springer-Verlag, NY, pp. 21-70, 1988.

[16] Bantam 3D Grass Application Web site: http://www.bantam3d.com

Authors' biographies

Oyundolgor KHORLOO received a BS degree in applied mathematics from National University of Mongolia in 1995 and an MS degree in computer science from University of Colorado at Denver in 2001. She is currently a PhD candidate in computer science at Iwate University. Her research interests include computer graphics, noise-based animation and simulation of natural phenomena.

Zorig GUNJEE is a researcher in ECM Co., Ltd, Mongolia. He received his bachelor's and master's degrees from Novosibirsk Technical University, Russia in 1986. He also got his master's degree in computer science from Mongolian University of Science and Technology in 2001 and his PhD degree from Iwate University, Japan in 2007. His research areas include point rendering, noise based animation, computer animation of natural phenomena, and graphics processing unit (GPU) programming.

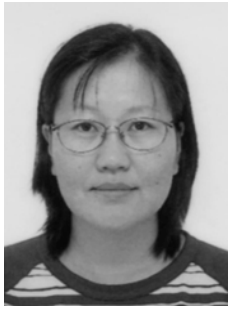

Batjargal SOSORBARAM is currently a research fellow in the Department of Computer Science at Iwate University. Her research interests include computer graphics and noise-based animation. She received a BE in science of physics from National University of Mongolia in 1988 and an ME and DE degrees in computer science from Iwate University in 1999 and 2003, respectively.

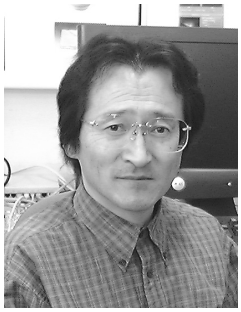

Norishige CHIBA is currently a Professor in Department of Computer Science at Iwate University. His research interests include Computer Graphics, Laser Graphics and Interactive Graphics. He received a BE in electrical engineering from Iwate University and an ME and DE in information engineering from Tohoku University in 1975, 1981 and 1984, respectively. He worked at Nippon Business Consultant Co., Ltd from 1975 to 1978. He was a research associate in the Department of Communication Engineering at Tohoku University from 1984 to 1986, an associate professor of Computer Science at Sendai National College of Technology from 1986 to 1987 and an associate professor of Computer Science at Iwate University from 1987 to 1991. He is a member of The Society for Art and Science, IEICE, IPS, IEEE and ACM.